Statistical modeling and optimization of *Escherichia coli* growth parameters for the biological treatment of phenol

Hayette Bouchene, Julien G. Mahy, Stéphanie D. Lambert, Bahdja Hayoun, Ourida Deflaoui, Mustapha Bourouina, Khaldoune Bachari, Adhya-Eddine Hamitouche, Saliha Bacha-Bourouina

PII: S1878-8181(21)00112-2

DOI: https://doi.org/10.1016/j.bcab.2021.102016

Reference: BCAB 102016

To appear in: *Biocatalysis and Agricultural Biotechnology*

Received Date: 23 February 2021

Revised Date: 23 April 2021

Accepted Date: 26 April 2021

Please cite this article as: Bouchene, H., Mahy, J.G., Lambert, S.D., Hayoun, B., Deflaoui, O., Bourouina, M., Bachari, K., Hamitouche, A.-E., Bacha-Bourouina, S., Statistical modeling and optimization of *Escherichia coli* growth parameters for the biological treatment of phenol, *Biocatalysis and Agricultural Biotechnology*, https://doi.org/10.1016/j.bcab.2021.102016.

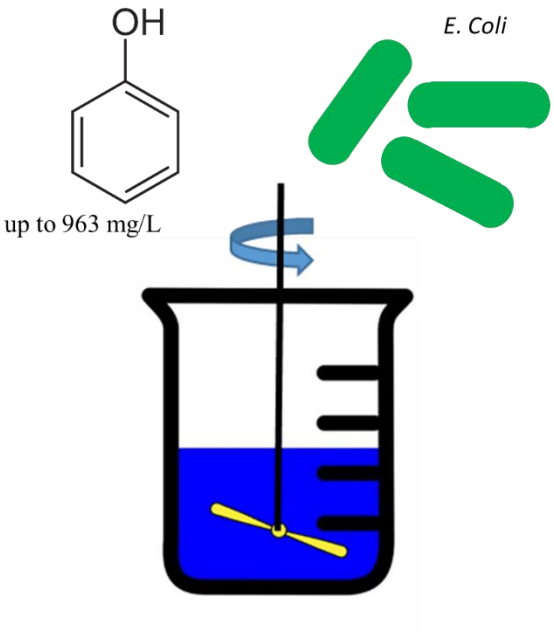

Biodegradation process optimization thanks to Baranyi and Roberts' equations :

Study of pH, initial concentrations of ammonium sulfate and phenol on growth parameters: latency time, λ (h), maximum specific growth rate, μ_{max} (h^{-1}), and maximum optical density, OD_{max}

Optimized parameters:

λ_{min} = 21.08 h, μ_{max} = 8.68 h^{-1} and OD_{max} = 0.39 at pH = 6.3 for $[phenol]_0$ = 200 mg/L and $[(NH_4)_2SO_4]_0$=1.33 g/L

Statistical modeling and optimization of *Escherichia coli* growth parameters for the biological treatment of phenol

Hayette Bouchene[1], Julien G. Mahy[2]*, Stéphanie D. Lambert[3], Bahdja Hayoun[4], Ourida Deflaoui[1], Mustapha Bourouina[4], Khaldoune Bachari[5], Adhya-Eddine Hamitouche[5], Saliha Bacha-Bourouina[1]

[1]*Faculté de Technologie, Département de Génie des Procédés, Université de Bejaia, 06000, Algeria.*

[2]*Institute of Condensed Matter and Nanosciences (IMCN), Université catholique de Louvain, Place Louis Pasteur 1, B-1348 Louvain-la-Neuve, Belgium*

[3]*Department of Chemical Engineering - Nanomaterials, Catalysis & Electrochemistry, University of Liège, B6a, Quartier Agora, Allée du six Août 11, 4000 Liège, Belgium.*

[4]*Faculté des Sciences Exactes, Département de Chimie, Université de Bejaia, 06000, Algeria*

[5]*Centre de Recherche Scientifique & Technique en Analyses Physico-Chimiques (CRAPC), BP 384, Zone Industrielle, Bou-Ismail RP, DZ-42004 Tipaza, Algeria*

***Corresponding author:** Julien G. Mahy, Institute of Condensed Matter and Nanosciences (IMCN), Université catholique de Louvain, Place Louis Pasteur 1, B-1348 Louvain-la-Neuve, Belgium. E-mail address: julien.mahy@uclouvain.be.

Abstract

Aromatic compounds, including phenols, are a significant source of pollution which need to be treated by environmentally-friendly methods, such as bioprocesses. This work focuses on the biodegradation of phenol in a batch reactor with bacteria, and the optimization of the growth parameters in order to obtain the highest phenol degradation. The model and

algorithms fitting the growth data are emphasized. Primary models, applied to monitor the dynamic evolution of the microbial biomass of the selected strain, were fitted to the data by nonlinear regression based on the Levenberg Marquart algorithm. The statistically-validated Baranyi and Roberts equation was used to evaluate the growth parameters: maximum growth rate (μ_{max}), latency time (λ), and maximum optical density (OD_{max}). To improve bacterial growth and phenol degradation performance, physico-chemical conditions, such as initial phenol concentration, pH, and nitrogen source (ammonium sulfate), were optimized using secondary models based on a central composite rotatable design (CCRD). The correlation coefficient, R^2, for each regression equation is > 94%. The optimal values of growth parameters are λ_{min} = 21.08 h, μ_{max} = 8.68 h^{-1}, and OD_{max} = 0.39 at pH = 6.3 for an initial concentration of phenol = 200 mg/L and initial concentration of ammonium sulfate = 1.33 g/L. *Escherichia coli* showed an ability to degrade up to 963 mg/L of phenol in 250 h without prior acclimatization of the strain.

Keywords: Phenol biodegradation; *Escherichia coli*; statistical modeling; Baranyi and Roberts model; central composite rotatable design.

1. Introduction

The treatment of environmental pollution is one of the major concerns of the 21st century, especially water pollution which has been of great importance for the last four decades. Aromatic compounds, including phenolic compounds, are known for their omnipresence in industrial effluents.

The toxicity of these products requires their elimination from water before it is discharged into rivers (Nair et al., 2008). Phenol is a basic reagent (Basha et al., 2010) used in numerous processes, such as coal processing plants (Pradeep et al., 2015; Zhai et al., 2012), petroleum

refineries, pulp and paper mills, iron and steel industries, plastics and varnishes, textile mills, pesticide factories, companies producing polymer resins, pharmaceutical industries, fiberglass manufacturing, and wood preservation plants (Al-Khalid and El-Naas, 2012; Iqbal et al., 2017; Ke et al., 2018; Zou et al., 2018). Acute exposure to phenol is known to cause gastrointestinal discomfort and headaches (Pradeep et al., 2015). Also, phenol is toxic to the nervous system, heart, kidneys, and liver and is easily absorbed through the skin (Zhai et al., 2012). Similarly, for aquatic organisms, phenol and its derivatives are toxic or lethal at concentrations from 5 to 25 mg/L (Al-Khalid and El-Naas, 2012).

Because of this toxicity, the Algerian regulations in accordance with Executive Decree No. 09-209 of June 11, 2009, describing the procedure for granting authorization to discharge non-domestic wastewater into a public sewerage network or a wastewater treatment plant, set 1 mg/L as the maximum limit for phenol content in this non-domestic wastewater. Also, Algerian Executive Decree No. 06-141 of April 19, 2006, defining the limit values for discharges of industrial liquid effluents, stipulated a value of 0.3 mg/L of effluents from the energy industry. Finally, the World Health Organization has established a guideline of 1 μg/L to regulate the concentration of phenol in drinking water, and a more severe guideline of 0.5 μg/L was set by the European Council's Drinking Water Directive. Moreover, the United States Environmental Protection Agency has defined phenol as a priority pollutant.

To comply with these standards of rejection, several physical or chemical treatment methods are available, such as activated carbon adsorption, ion exchange, liquid-liquid extraction, or chemical oxidation (Al-Khalid and El-Naas, 2012). Unfortunately, these methods often suffer from drawbacks, such as high cost, or they simply transfer the pollution from one phase to another (e.g., from the liquid water to a solid such as carbon) (Al-Khalid and El-Naas, 2012).

In contrast, biological processes (using microorganisms for phenol degradation) are more attractive because they are considered to be more environmentally friendly (Koyande et al.,

2019; Tang et al., 2020; Yew et al., 2021) and more economical than chemical and physical treatments (Chai et al., 2021; Ke et al., 2018; Pradeep et al., 2015; Rambabu et al., 2020; Show et al., 2012; Tang et al., 2020; Xie et al., 2021, 2020; Zhai et al., 2012). Several microorganisms (bacteria, fungi, yeasts, and microalgae) were studied for the biodegradation of phenol (Basha et al., 2010; Lindner and Pleissner, 2019; Singh and Kumar, 2019). These microorganisms use the phenol as a carbon source for their development during cell growth, as phenol is the only source of carbon present in the medium. A biodegradation study cannot be carried out without optimizing the kinetic parameters of the growth of the microorganisms responsible for the degradation of phenol in order to ensure good microorganism development. To highlight some of the relationships between all the different parameters, statistical experimental designs provide the best methodologies to optimize and evaluate the factors that influence the biodegradation process of phenol (Presser et al., 1997; Tebbouche et al., 2015).

The aim of this study is to evaluate the capacity for phenol biodegradation of *Escherichia coli RV412_A1_A1_2010_06a LBK* isolated from the wastewater treatment plant of Beni Messous (Algeria). First, a central composite rotatable design (CCRD) was chosen to study the influence of three factors, namely pH, the initial phenol concentration, and initial nitrogen source concentration on the growth kinetics of the isolated bacteria during phenol degradation. The bacterial growth parameters, such as maximum growth rate (μ_{max}), latency time (λ), and maximum optical density (OD_{max}), were previously estimated using two primary models widely applied in microbiology: Gompertz, and Baranyi and Roberts. The polynomial regression equations are established for these kinetic growth parameters as a function of the three factors and their interactions. The second part of this work concerns the study of the influence of the operating factors on the phenol degradation yield and its relation to the

evolution of bacterial growth parameters. This bacterial strain can be applied for the treatment of highly concentrated solutions of phenol (up to 1000 mg/L).

2. Methods

2.1. Microorganism type and culture conditions

The bacterial strain used in this work was collected and isolated from the Wastewater Treatment Plant of Beni Messous station (Algiers, Algeria). The bacterial culture was stored at 4°C. For all experiments, the cultured biomass was inoculated into 100 mL of culture medium for 24 h at 30°C and recovered by centrifugation (3000 rpm for 30 min) (Hamitouche et al., 2010). The culture medium was composed of peptone (15 g/L), yeast extract (3 g/L), sodium chloride (6 g/L), and (D+)-glucose (1 g/L). The biomass obtained was rinsed with a 0.5% NaCl solution and centrifuged again. The rinsed microorganisms were then suspended in 0.5% NaCl (Hamitouche et al., 2010). All cultures were carried out at 1% V/V at an initial OD_{600nm} = 0.09.

2.2. Identification of the bacteria

The identification of the bacteria was achieved by mass spectroscopy (Labella et al., 2021; Sun et al., 2021) thanks to the matrix assisted laser desorption ionization - time of flight (MALDI-TOF) technique using a device from Bruker Daltonik (Billerica, MA, USA). The mass spectrum obtained was compared to a database of reference spectra (RUO MALDI Biotyper Reference Library v3.3.1.2, SR library v1.0) by the software (Bruker Daltonik) to determine relatedness to spectra in the database (Shah and Gharbia, 2017).

~~The principle of mass spectroscopy is the detection and identification of molecules according to their mass and the characterization of their chemical structure by gas separation of ions according to their m/Z ratio. MALDI-TOF is a technique of ionization of biomolecules. This~~

~~method involves three major steps: (i) deposition of the sample on a metal plate by mixing it with a matrix which crystallizes it, (ii) ionization by bombardment with brief laser pulses, producing positively charged analytes, (iii) separation of ions formed by this process according to their TOF in the flight tube. Ion collisions in the flight tube are avoided by the generation of a vacuum pushed by a pump, before the laser pulses, which takes 1-2 min. Protein detection at the exit of flight tube leads to the production of a mass spectrum composed of specific mass peaks with different intensities that express a reproducible fingerprint of a microorganism. At the end of the analysis, the spectra obtained are compared with reference databases (Shah and Gharbia, 2017).~~

2.3. Biodegradation of phenol

The biodegradation experiments were carried out under aseptic conditions, 1 mL of the conserved culture was inoculated into 100 mL of Nutrient Broth Medium and incubated for 24 h at 30°C. The resulting biomass was suspended in NaCl 0.5% solution as previously described. The initial density was measured by spectrophotometry at 600 nm, and was equal to 2.5 to 2.9. When inoculated into a 250 mL Erlenmeyer flask containing 100 mL saline medium, $OD_{600\ nm} = 0.09$.

The composition of the culture medium was (g/L): NaH_2PO_4: 3, KH_2PO_4: 3, $MgSO_4$: 0.1, and the nitrogen source ($(NH_4)_2SO_4$) was optimized in the range of 0 to 2 g/L, the carbon source (phenol) varied in the range of 50 to 200 mg/L. pH was optimized within the range of 6 to 8. All experiments were performed at 30°C. Similarly, the effect of the initial phenol concentration (65, 562, and 963 mg/L) on microorganism growth and phenol degradation was examined.

2.4. Design of the experiments

The modeling and optimization of the responses were carried out using a central composite rotatable design (CCRD) provided by the software Minitab 17. This design was chosen to evaluate the main effects and the interactions of three parameters: the initial concentration of phenol (50 to 200 mg/L), $[phenol]_0$, the initial concentration of ammonium sulfate (0 to 2 g/L), $[(NH_4)_2SO_4]_0$, and pH (6 to 8), on three responses: the latency time, λ (h), the maximum specific growth, μ_{max} (h^{-1}), and the maximum optical density, OD_{max}. The statistical significance of these models was evaluated using analysis of variance (ANOVA).

The correlations between the operating variables (pH, $[(NH_4)_2SO_4]_0$, and $[phenol]_0$) and the responses were estimated by a full quadratic model (Eq. 1):

$$Y = b_0 + b_1 x_1 + b_2 x_2 + b_3 x_3 + b_{12} x_1 x_2 + b_{13} x_1 x_3 + b_{23} x_2 x_3 + b_{11} x_1^2 + b_{22} x_2^2 + b_{33} x_3^2 + \ldots \quad \text{(Eq. 1)}$$

where b_0 is constant and is defined as the response mean, b_j represents the linear effects with i=1, 2, or 3, and b_{jj} represents the interaction effects with i=1, 2, or 3 and j=1, 2, or 3.

The growth parameters (the latency time, λ (h), the maximum specific growth, μ_{max} (h^{-1}), and the maximum optical density, OD_{max}) were determined for each iteration of the design using the most appropriate primary model.

2.5. Kinetic models of growth

Growth curves were simulated using two primary models, the modified Gompertz model (Eq. 2) and the Baranyi and Roberts model (Eq. 3) (Imadalou-Idres et al., 2018; Romano et al., 2007). The cell quantification was expressed in terms of optical density at 600 nm,

173 analyzed by spectrophotometry (Baranyi et al., 1993; Lopez et al., 2004; Zwietering et al.,
174 1990):
175

176 $$\ln N = \ln N_0 + A\, e^{-e^{\left\{\left(\frac{\mu_{max} e^{1}}{A}\right)(\lambda-1)\right\}+1}} \quad \text{(Eq. 2)}$$

177 $$\ln N = \ln N_0 + \mu_{max} t + \ln\left[e^{-\mu_{max} t} - e^{-\mu_{max}(t+\lambda)} + e^{-\mu_{max}\lambda}\right] - \ln\left[1 + \frac{\left(e^{\mu_{max}(t-\lambda)} + e^{-\mu_{max}\lambda}\right)}{e^{(\ln N_{max} - \ln N_0)}}\right] \quad \text{(Eq. 3)}$$

178

179 where N denotes the microbial biomass measured at time t; N_0 and N_{max} are the microbial
180 biomass measured at t = 0 and at maximum microbial population size, respectively; A is the
181 asymptotic level = $\ln\left(\frac{N_{max}}{N_0}\right)$; μ_{max} is the maximum specific growth rate (h^{-1}), and is defined as
182 the tangent to the inflection point of the growth curve; λ is the latency phase duration (h); t is
183 time (h).
184

185 **2.6. Analytical methods**

186 The residual phenol was quantified by applying the colorimetric method by complexation of
187 phenol with potassium ferricyanide (Yang and Humphrey, 1975). For the colorimetric
188 quantification of phenol, 1.15 mL NaAc-HAc buffer (0.2 M, pH 4.0) and 100 μL potassium
189 ferricyanide (0.5 mg mL^{-1}) were first mixed together, and then 900 μL phenol at different
190 concentrations was added to the above solution (Yang and Humphrey, 1975). After incubation
191 at room temperature for 30 min, the system was measured by using a visible
192 spectrophotometer Hammatsu at 510 nm (Rodier and Legube, 2009).
193

194 **3. Results and discussion**

3.1. Identification of biomass

In this study, the bacterial strain used was isolated from a wastewater treatment plant. Before proceeding with the modeling and optimization of biodegradation processes, it is necessary to start by identifying the isolated strain using MALDI-TOF spectroscopy, a method based on the analysis of the protein composition produced by the analyzed sample (Asakawa et al., 2013).

Two reproducible MALDI-TOF spectra were obtained for two different samples (Figure 1). Comparison of these spectra with the database of reference spectra (RUO MALDI Biotyper Reference Library v3.3.1.2, SR library v1.0) revealed that the bacterial strain is an *Escherichia coli RV412_A1_2010_06a LBK* with a value equal to 2.259 (Schoch et al., 2020). The closer this score value is to 3, the higher the probability of species identification accuracy.

3.2. Kinetic model

The curve of Figure 2 shows the growth of *E. coli* bacteria in aerobic conditions at 30°C and medium containing (g/L): NaH_2PO_4: 3, KH_2PO_4: 3, $MgSO_4$: 0.1, $(NH_4)_2SO_4$: 1, and phenol as the sole source of carbon at an initial concentration equal to 125 mg/L. Three distinct growth phases are observed: (i) the latency period, which serves to adapt the inoculum (N_0) to its new environment. During this period, the specific growth rate is equal to zero ($\mu = 0$); (ii) the exponential phase where specific growth rate of the bacteria is maximum ($\mu = \mu_{max}$); (iii) the stationary period, for which the growth rate is equal to zero ($\mu = 0$) and the culture reaches its maximum density ($N = N_{max}$) (Imadalou-Idres et al., 2018).

The growth curves obtained for the various operating conditions follow the models currently applied in microbiology, such as the Gompertz model (Imadalou-Idres et al., 2018) or Baranyi and Roberts model (Romano et al., 2007). The parameters of these models were estimated by

fitting curves to experimental growth data by nonlinear regression (Minitab 17). Both models have previously been successfully applied to the modeling of *Escherichia coli* growth curves (Fujikawa et al., 2004; Lopez et al., 2004).

Table 1 represents the analysis of variance for the Gompertz and Baranyi and Roberts primary models. The values of coefficients R^2 and RMSE are very similar between both models. As the Baranyi and Roberts model presents more advantageous statistical properties compared to the Gompertz model, the Baranyi and Roberts model was chosen to calculate the kinetic parameters of bacterial growth.

3.3. Central composite rotatable design evaluation

The bacteria used in this work showed an ability to degrade phenol. To understand this process, three parameters influencing growth kinetics were studied: pH of the solution, the initial concentration of ammonium sulfate, $[(NH_4)_2SO_4]_0$, and the initial concentration of phenol, $[phenol]_0$. The growth parameters, latency time, λ, the maximum specific growth rate, μ_{max}, and the maximum optical density, OD_{max}, were determined for nineteen experimental points. For each test, the experimental parameter was set at one level and the other two at their different levels in the field of study, for all possible combinations. Table 2 presents the factors and levels used in the central composite rotatable design, and the experimental matrix is shown in Table 3.

Figure 3 presents the kinetic parameters λ, μ_{max}, and OD_{max} calculated by the Baranyi and Roberts model. The results of the matrix, shown in Table 3, were analyzed using the statistical program Minitab 17, running on Windows 7. The coefficients of a quadratic polynomial model were estimated by multiple regression using the least squares method. The main, quadratic, and interaction effects, and the *P*-value corresponding to the Fisher-Snedecor test are listed in Table 4. The significance of each coefficient shown in Table 4 was checked by its

P-value: if the *P*-value < 0.05, the coefficient is significant, if the *P*-value > 0.05, the coefficient does not contribute to the change of the response studied and was removed from the regression equation. Coefficients with positive signs contribute to increase the studied response and coefficients with negative signs reduce it. The quality of the predicted model is evaluated by the coefficient of determination and the analysis of variances makes it possible to estimate whether the predicted model is significant and adequate (Goupy and Creighton, 2006).

The *P*-value for the three models (0.000 for λ, 0.012 for OD_{max}, and 0.000 for μ_{max}) indicate that the quadratic regression equations are significant and adequate. Also, the *P*-value due to the lack of fit is > 0.05 (Table 1, Run 0) which indicates that the models have no bias. This result is confirmed by comparing the values of the responses calculated by the model with those obtained experimentally (Figure 3). The R^2 values > 94 % (Table 5) for λ, OD_{max}, and μ_{max}, are explained by the corresponding regression. The equations for the three responses in uncoded units (after eliminating the insignificant effects and recalculating the new coefficients) are given by:

$$\lambda = 4763 - 1116\ pH - 839.6\ [(NH_4)_2SO_4]_0 - 4.893\ [phenol]_0 + 59.82\ [pH]^2 + 99.88\ [(NH_4)_2SO_4]_0^2 - 0.01085\ [phenol]_0^2 + 90.98\ pH\ [(NH_4)_2SO_4]_0 + 1.192\ pH\ [phenol]_0 \quad \text{(Eq. 4)}$$

$$\mu_{max} = -78.98 + 14.1\ pH - 12.47\ [(NH_4)_2SO_4]_0 + 0.5819\ [phenol]_0 + 0.000281\ [phenol]_0^2 - 0.11019\ pH\ [phenol]_0 + 0.10083\ [(NH_4)_2SO_4]_0\ [phenol]_0 \quad \text{(Eq. 5)}$$

$$OD_{max} = 3.34 - 0.925\ pH - 0.0866\ [(NH_4)_2SO_4]_0 + 0.001213\ [phenol]_0 + 0.0657\ [pH]^2 + 0.0553\ [(NH_4)_2SO_4]_0^2 \quad \text{(Eq. 6)}$$

Microbial kinetics depend on several factors, including those chosen for the design of the experiment. In Eq. 4, pH has a negative effect on the response, so any increase in this parameter reduces the latency time. Similar results were found by Buchanan and Klawitter (1992) who studied the effect of the initial pH on the lag phase duration of the growth of bacteria *E. coli 0157:H7* in the presence of NaCl. In this study, there is a different Na-containing compound present, NaH_2PO_4, but nevertheless, the bacteria seem to be better suited to an alkaline or neutral environment compared to an acidic environment. This effect is well illustrated in Figure 4.

The increase in the initial concentration of phenol is favorable within a certain limit, it is generally known that biodegradation by microbial cells is inhibited by phenol itself, particularly at higher concentrations, and the latency period increases with the initial concentration of phenol (Goupy and Creighton, 2006; Hamitouche and Bendjama, 2012) (Figure 4). It can be seen in Figure 4 that the initial phenol content has a negative effect and delays the maximum specific growth rate. Nevertheless, the highest OD_{max} value is obtained for the higher initial phenol concentration.

The effect of the interactions is relative to the combined influence of the two parameters in question. In Figure 5, it is observed that even if the initial concentration of $(NH_4)_2SO_4$ has no effect on the latency period, its interaction with the effect of pH has a positive effect on the response. Also, the pH and initial concentration of phenol interactions have a positive effect on the latency period.

In addition, the pH has no significant effect on the maximum specific growth rate in the studied domain, but its interaction with the initial concentration of phenol has a negative effect. In contrast, the interaction $[(NH_4)_2SO_4]_0$*$[phenol]_0$ has a positive effect on μ_{max}, so to

optimize this response, it is necessary to vary these last two factors in the same direction. These results are represented in Figure 5.

The equations 4, 5, and 6 were used to draw the contour plots to define the effects of the different factors on λ, OD_{max}, and μ_{max}. The contour plots in Figure 6 are useful for determining desirable response values and operating conditions. The contour areas represent constant responses, which correspond to μ_{max} varying from 0.1 up to 10 (h^{-1}), OD_{max} between 0.1 to 0.5, and λ going up to 200 h. The contours with the darkest green color indicate the zone where response is the highest, while those with the darkest blue correspond to the weakest responses.

It is remarkable that μ_{max} is dependent on the pH*$[(NH_4)_2SO_4]_0$ interaction, the highest value is obtained in the areas corresponding to the upper left corner of the chart. This plot suggests that it is possible to maximize OD_{max} and μ_{max} or minimize λ under certain values of pH, initial nitrogen, and phenol concentrations. The contours suggest that the response surface is a rising ridge. Note that whatever the nitrogen concentration, these contours are identical, *i.e.*, the nitrogen concentration does not influence this response.

The interaction pH*$[phenol]_0$ is not significant for OD_{max} but highly significant for λ and μ_{max}. The highest growth rates are achieved at pH = 6 for the solutions with the highest initial phenol concentration and at pH = 8 for solutions with lower initial phenol concentrations.

In Figure 6, the darkest green region is observed only in the upper right corner of the contour curves of the OD_{max} response when the specific growth rate is maximum for solutions with the highest initial concentrations of phenol and ammonium sulfate. It is also noted on the contour diagram that the smallest latency value (λ = 1 h) is obtained for the following conditions:

- For neutral pH, in the solution with 1 g/L of ammonium sulfate and 50 mg/L of phenol

Also, in the same logic, the optimal values for μ_{max} can be estimated for:

- pH = 6, in the solution with 2 g/L of ammonium sulfate and 200 mg/L of phenol

The contour curves for OD_{max} indicate that the optimum is obtained at pH = 6 for an initial phenol concentration equal to 200 mg/L and for an initial ammonium sulfate content equal to 2 g/L, similar values to those corresponding to μ_{max}.

The optimal values for *E. coli* growth parameters are: λ_{min} = 21.08 h, μ_{max} = 8.68 h^{-1} and OD_{max} = 0.39 at pH = 6.3 for $[phenol]_0$ = 200 mg/L and $[(NH_4)_2SO_4]_0$ = 1.33 g/L, values given by the Minitab Software 17.

3.4. Effect of initial phenol concentration

For the initial concentrations of phenol equal to 562 and 963 mg/L, bacterial growth and the residual concentration of phenol (Figure 7a) were monitored as a function of time. In agreement with previous works (Câmara et al., 2019; Hamitouche and Bendjama, 2012; Peng et al., 2018; Stoilova et al., 2006; Wang et al., 2019), the increase of the initial concentration of phenol automatically leads to the increase of the biomass produced at the end of the exponential phase.

The effect of the initial phenol concentration on the latency period is shown in Figure 7b. It is observed that the latency time increases with initial phenol concentration, which leads to the conclusion that the substrate has an inhibitory effect on the growth of bacteria (Ucun et al., 2010).

The results presented in this work are innovative. While most of the previous works first acclimatize the microorganisms to varying concentrations of phenol before carrying out the biodegradation tests, all the growth curves recorded in this work are obtained for cultures of bacteria taken directly without prior acclimatization. This is only the second work that deals with an *E. coli* strain that is able to biodegrade phenol without acclimatization, the other being Fayidh et al. (2015).

4. Conclusions

This study demonstrated the ability of *Escherichia coli RV412_A1_2010_06a LBK* to remove different phenol concentrations up to 963 mg/L. Modeling using the Surface Response Methodology was performed to study the effects of pH and initial concentrations of ammonium sulfate and phenol on growth parameters (latency time, λ (h), maximum specific growth rate, μ_{max} (h^{-1}), and maximum optical density, OD_{max}). Second order models were developed to predict growth parameters. Thanks to ANOVA software, it has been statistically demonstrated that approximately 98.8%, 99.6%, and 94.5% of the responses for μ_{max}, λ, and OD_{max} respectively are explained by the regression equations of these models. The optimal values of growth parameters are λ_{min} = 21.08 h, μ_{max} = 8.68 h^{-1}, and OD_{max} = 0.39 at pH = 6.3 for $[phenol]_0$ = 200 mg/L and $[(NH_4)_2SO_4]_0$ =1.33 g/L. As a result of this work, this strain will be acclimatized to large amounts of phenolic pollutants and other more pathogenic pollutants such as pharmaceutical compounds in a future work.

Acknowledgements:

S. D. L. is grateful to F.R.S.-F.N.R.S. for her Senior Research Associate position. The authors also acknowledge the Ministère of Algeria for financial support.

Compliance with ethical standards

Conflict of interest: the authors declare that they have no conflicts of interest.

Data availability

The raw/processed data required to reproduce these findings cannot be shared at this time as the data also forms part of an ongoing study.

369

370 **References**

371 Al-Khalid, T., El-Naas, M.H., 2012. Aerobic Biodegradation of Phenols : A Comprehensive
372 Review. Crit. Rev. Environ. Sci. Technol. 42, 1631–1690.
373 https://doi.org/10.1080/10643389.2011.569872

374 Asakawa, D., Bernevic, B., Cai, Z., Debois, D., Demeure, K., De Pauw, E., Erba, E.B., Gao,
375 X., Guo, Y., He, Z., Liu, N., Liu, S., Lu, M., Ma, L., Mädler, S., Przybylski, M., Qi,
376 R.Z., Quinton, L., Schellander, K., Smargiasso, N., Sugrue, R.J., Susnea, I., Tang, K.,
377 Tan, B.H., Wang, H., Wicke, M., Yang, H., Yu, W., Zenobi, R., Zhao, Z., Zimmerman,
378 T.A., 2013. Applications of MALDI-TOF Spectroscopy, Topics in. ed. Springer,
379 London.

380 Baranyi, J., Mcclure, P.J., Sutherland, J.P., Roberts, T.A., 1993. Modeling bacterial growth
381 responses. J. Ind. Microbiol. 12, 190–194.

382 Basha, K.M., Rajendran, A., Thangavelu, V., 2010. Recent advances in the Biodegradation of
383 Phenol: A review. Asian J. Exp. Biol. Sci. 1, 219–234.

384 Buchanan, R.L., Klawitter, L.A., 1992. The effect of incubation temperature , initial pH , and
385 sodium chloride on the growth kinetics of Escherichia coli 0157:H7. Food Microbiol. 9,
386 185–196.

387 Câmara, N., Casimiro, A., Macedo, D., Daniel, Á., Pinheiro, T., 2019. Journal of
388 Environmental Chemical Engineering Phenol biodegradation by Candida tropicalis
389 ATCC 750 immobilized on cashew apple bagasse. J. Environ. Chem. Eng. 7, 103076.
390 https://doi.org/10.1016/j.jece.2019.103076

391 Chai, W.S., Tan, W.G., Unawaroh, H.S.H., Gupta, V.K., Ho, S., Show, P.L., 2021.
392 Multifaceted roles of microalgae in the application of wastewater biotreatment : A
393 review *. Environ. Pollut. 269, 116236. https://doi.org/10.1016/j.envpol.2020.116236

394 Fayidh, M.A., Sabina, K., Sudharsan, K., Sukumar, M., 2015. Isolation of a unique Phenol
395 degrading bacterial strain Escherichia coli moh 1 from effluent of an edible oil industry
396 in Chennai , India. Res. J. Biotechnol. 10, 36–42.

397 Fujikawa, H., Kai, A., Morozumi, S., 2004. A new logistic model for Escherichia coli growth
398 at constant and dynamic temperatures. Food Microbiol. 21, 501–509.
399 https://doi.org/10.1016/j.fm.2004.01.007

400 Goupy, J., Creighton, L., 2006. Introduction aux plans d'expériences-3ème édition. Hachette.

401 Hamitouche, A., Amrane, A., Bendjama, Z., Kaouah, F., 2010. Effect of the Ammonium
402 Chloride Concentration on the Mineral Medium Composition – Biodegradation of
403 Phenol by a Microbial Consortium. Int. J. Environ. Res. 4, 849–854.

404 Hamitouche, A., Bendjama, Z., 2012. Relevance of the Luong model to describe the
405 biodegradation of phenol by mixed culture in a batch reactor. Ann. Microbiol. 62, 581–
406 586. https://doi.org/10.1007/s13213-011-0294-6

407 Imadalou-Idres, N., Boudrioua, A., Bacha-Bourouina, S., Benallaoua, S., 2018.
408 OPTIMIZATION OF PHYSICO-CHEMICAL CONDITIONS FOR GROWTH AND

ANTI-ARCHAEAL PRODUCTION BY Haloarcula sp. SWO25 Nacéra Imadalou - Idres* 1 , AbdelHakim Boudrioua 1 , Saliha Bacha-Bourouina 2 and Said Benallaoua 1. J. Microbiol. Food Sci. 7, 524–531. https://doi.org/10.15414/jmbfs.2018.7.5.524-531

Iqbal, A., Arshad, M., Hashmi, I., Karthikeyan, R., Gentry, T.J., Schwab, A.P., 2017. Biodegradation of Phenol and Benzene by Endophytic Bacterial Strains Isolated from Refinery Wastewater-Fed Cannabis sativa. Environ. Technol. 39, 1705–1714. https://doi.org/10.1080/09593330.2017.1337232

Ke, Q., Zhang, Yunge, Wu, X., Su, X., Wang, Y., Lin, H., Mei, R., Zhang, Yu, Za, M., Chen, C., Chen, J., 2018. Sustainable biodegradation of phenol by immobilized Bacillus sp . SAS19 with porous carbonaceous gels as carriers. J. Environ. Manage. 222, 185–189. https://doi.org/10.1016/j.jenvman.2018.05.061

Koyande, A.K., Chew, K.W., Rambabu, K., Tao, Y., Chu, D., Show, P., 2019. Microalgae : A potential alternative to health supplementation for humans. Food Sci. Hum. Wellness 8, 16–24. https://doi.org/10.1016/j.fshw.2019.03.001

Labella, A., Molero, R., Leiva-rebollo, R., Pérez-recuerda, R., Borrego, J.J., 2021. Science of the Total Environment Identification , resistance to antibiotics and bio film formation of bacterial strains isolated from a reverse osmosis system of a drinking water treatment plant. Sci. Total Environ. 774, 145718. https://doi.org/10.1016/j.scitotenv.2021.145718

Lindner, A.V., Pleissner, D., 2019. Utilization of phenolic compounds by microalgae. Algal Res. 42, 101602. https://doi.org/10.1016/j.algal.2019.101602

Lopez, S., Prieto, M., Dijkstra, J., Dhanoa, M.S., France, J., 2004. Statistical evaluation of mathematical models for microbial growth. Int. J. Food Microbiol. 96, 289–300. https://doi.org/10.1016/j.ijfoodmicro.2004.03.026

Nair, C.I., Jayachandran, K., Shashidhar, S., 2008. Biodegradation of phenol. African J. Biotechnol. 7, 4951–4958.

Peng, S.S., Ling, N.S., Rohana, A., 2018. Kinetics of Biodegradation of Phenol and p - nitrophenol by Acclimated Activated Sludge. J. Phys. Sci. 29, 107–113.

Pradeep, N. V, Anupama, S., Navya, K., Shalini, H.N., Idris, M., Hampannavar, U.S., 2015. Biological removal of phenol from wastewaters : a mini review. Appl. Water Sci. 5, 105–112. https://doi.org/10.1007/s13201-014-0176-8

Presser, K.A., Ratkowsky, D.A., Ross, T., 1997. Modelling the Growth Rate of Escherichia coli as a Function of pH and Lactic Acid Concentration. Appl. Environ. Microbiol. 63, 2355–2360.

Rambabu, K., Banat, F., Minh, Q., Ho, S., Ren, N., 2020. Environmental Science and Ecotechnology Biological remediation of acid mine drainage : Review of past trends and current outlook. Environ. Sci. Ecotechnology 2, 100024. https://doi.org/10.1016/j.ese.2020.100024

Rodier, J., Legube, B., 2009. L'analyse de l'eau. Dunod.

Romano, A., Toraldo, G., Cavella, S., Masi, P., 2007. Description of leavening of bread dough with mathematical modelling. J. Food Eng. 83, 142–148. https://doi.org/10.1016/j.jfoodeng.2007.02.014

Schoch, C.L., Ciufo, S., Domrachev, M., Hotton, C.L., Kannan, S., Khovanskaya, R., Leipe, D., Mcveigh, R., Neill, K.O., Robbertse, B., Sharma, S., Soussov, V., John, P., Sun, L., Turner, S., Karsch-mizrachi, I., 2020. NCBI Taxonomy : a comprehensive update on curation , resources and tools. Database 2020, 1–21. https://doi.org/10.1093/database/baaa062

Shah, H.N., Gharbia, S.E., 2017. MALDI - TOF and Tandem MS for Clinical Microbiology Edited by. John Wiley & Sons Ltd, Chichester.

Show, P.L., Tan, C.P., Anuar, M.S., Ariff, A., Yusof, Y.A., Chen, S.K., Ling, T.C., 2012. Bioresource Technology Extractive fermentation for improved production and recovery of lipase derived from Burkholderia cepacia using a thermoseparating polymer in aqueous two-phase systems. Bioresour. Technol. 116, 226–233. https://doi.org/10.1016/j.biortech.2011.09.131

Singh, P., Kumar, R., 2019. Critical Review of Microbial Degradation of Aromatic Compounds and Exploring Potential Aspects of Furfuryl Alcohol Degradation. J. Polym. Environ. 27, 901–916. https://doi.org/10.1007/s10924-019-01416-z

Stoilova, I., Krastanov, A., Stanchev, V., Daniel, D., Gerginova, M., Alexieva, Z., 2006. Biodegradation of high amounts of phenol , catechol , 2 , 4-dichlorophenol and 2 , 6-dimethoxyphenol by Aspergillus awamori cells. Enzyme Microb. Technol. 39, 1036–1041. https://doi.org/10.1016/j.enzmictec.2006.02.006

Sun, S., Huang, S., Shi, Y., Shao, Y., Qiu, J., Sedjoah, R.A., Yan, Z., Ding, L., Zou, D., Xin, Z., 2021. Extraction , isolation , characterization and antimicrobial activities of non-extractable polyphenols from pomegranate peel. Food Chem. 351, 129232. https://doi.org/10.1016/j.foodchem.2021.129232

Tang, D.Y.Y., Yew, G.Y., Koyande, A.K., Chew, K.W., Vo, D.-V.N., Show, P.L., 2020. Green technology for the industrial production of biofuels and bioproducts from microalgae : a review. Environ. Chem. Lett. 18, 1967–1985.

Tebbouche, L., Hank, D., Zeboudj, S., Namane, A., 2015. Evaluation of the phenol biodegradation by Aspergillus niger : application of full factorial design methodology. Desalin. Water Treat. 57, 6124–6130. https://doi.org/10.1080/19443994.2015.1053991

Ucun, H., Yildiz, E., Nuhoglu, A., 2010. Bioresource Technology Phenol biodegradation in a batch jet loop bioreactor (JLB): Kinetics study and pH variation. Bioresour. Technol. 101, 2965–2971. https://doi.org/10.1016/j.biortech.2009.12.005

Wang, Y., Meng, F., Li, H., Zhao, S., Liu, Q., Lin, Y., Wang, G., Wu, J., 2019. Biodegradation of phenol by Isochrysis galbana screened from eight species of marine microalgae : growth kinetic models , enzyme analysis and biodegradation pathway. J. Appl. Phycol. 31, 445–455.

Xie, B., Liang, H., You, H., Deng, S., Yan, Z., 2021. Chemosphere Microbial community dynamic shifts associated with sulfamethoxazole degradation in microbial fuel cells. Chemosphere 274, 129744. https://doi.org/10.1016/j.chemosphere.2021.129744

Xie, B., Tang, X., Yong, H., Deng, S., Shi, X., 2020. Biological sulfamethoxazole degradation along with anaerobically digested centrate treatment by immobilized microalgal-bacterial consortium : Performance , mechanism and shifts in bacterial and microalgal

communities. Chem. Eng. J. 388, 124217. https://doi.org/10.1016/j.cej.2020.124217

Yang, R. Der, Humphrey, A.E., 1975. Dynamic and Steady State Studies of Phenol Biodegradation in Pure and Mixed Cultures. Biotechnol. Bioeng. 17, 1211–1235.

Yew, G.Y., Tan, X., Wayne, K., Chang, J., Tao, Y., Jiang, N., Loke, P., 2021. Thermal-Fenton mechanism with sonoprocessing for rapid non-catalytic transesterification of microalgal to biofuel production. Chem. Eng. J. 408, 127264. https://doi.org/10.1016/j.cej.2020.127264

Zhai, Z., Wang, H., Yan, S., Yao, J., 2012. Biodegradation of phenol at high concentration by a novel bacterium : Gulosibacter sp . YZ4. J. Chem. Technol. Biotechnol. 87, 105–111. https://doi.org/10.1002/jctb.2689

Zou, S., Zhang, B., Yan, N., Zhang, C., Xu, H., Zhang, Y., Rittmann, B.E., 2018. Competition for molecular oxygen and electron donor between phenol and quinoline during their simultaneous biodegradation. Process Biochem. 70, 136–143. https://doi.org/10.1016/j.procbio.2018.04.015

Zwietering, M.H., Jongenburger, I., Rombouts, F.M., Van't Riet, K., 1990. Modeling of the Bacterial Growth Curve. Appl. Environ. Microbiol. 56, 1875–1881.

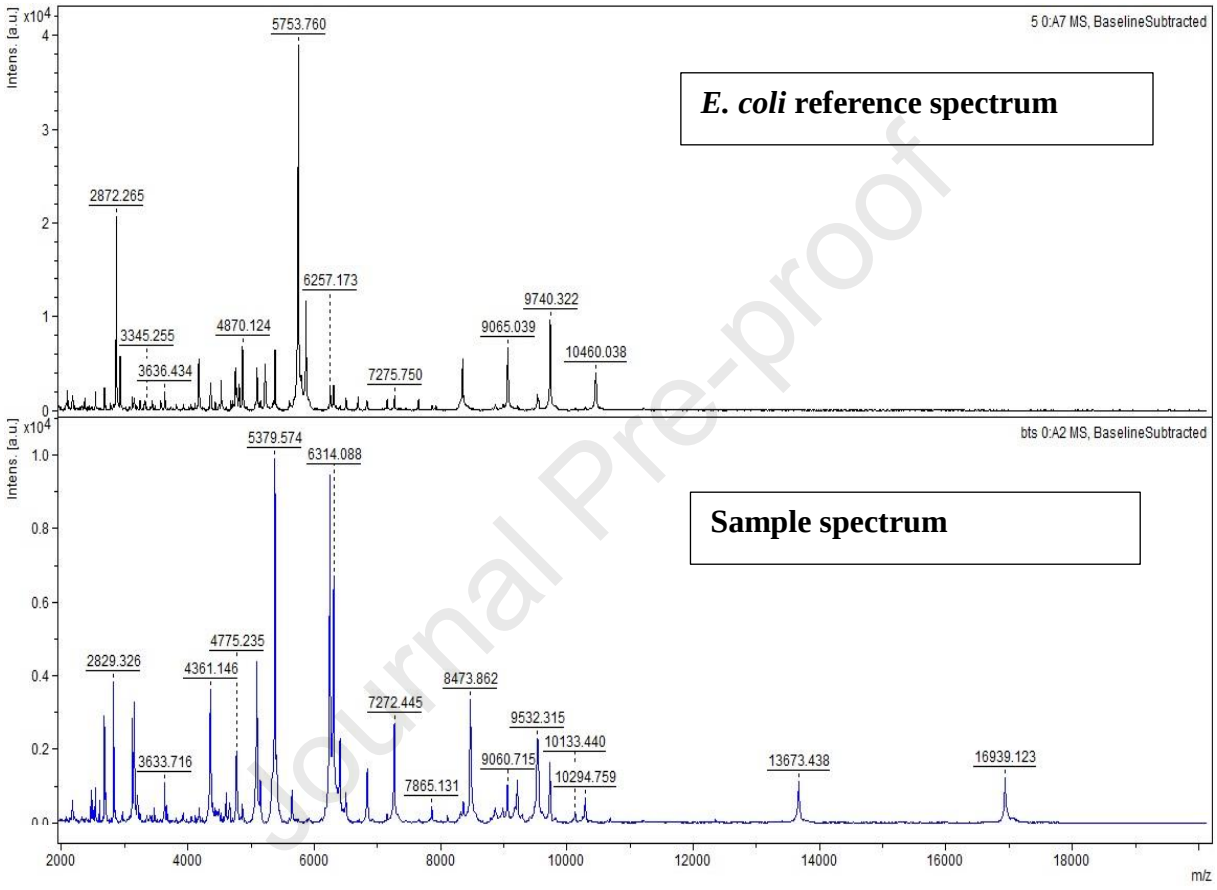

Figure 1: Matrix assisted laser desorption ionization - time of flight (MALDI-TOF) spectrum obtained from study samples compared to *Escherichia coli* reference spectrum.

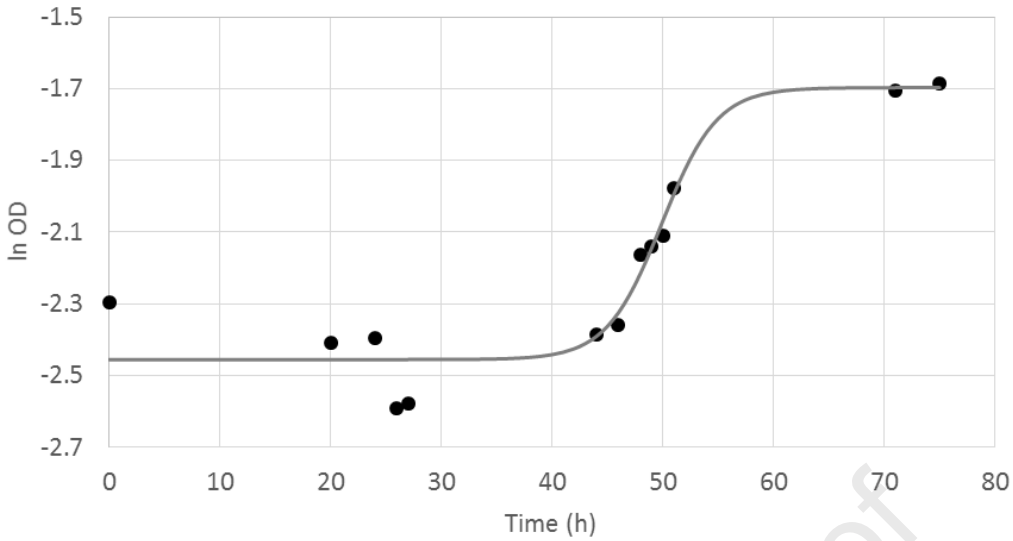

549

550 **Figure 2:** Growth curve of *Escherichia coli* at 30°C fitted with the Baranyi and Roberts
551 model (Imadalou-Idres et al., 2018; Romano et al., 2007), OD = optical density.

552

553

554

555

556

557

558

559

560

561

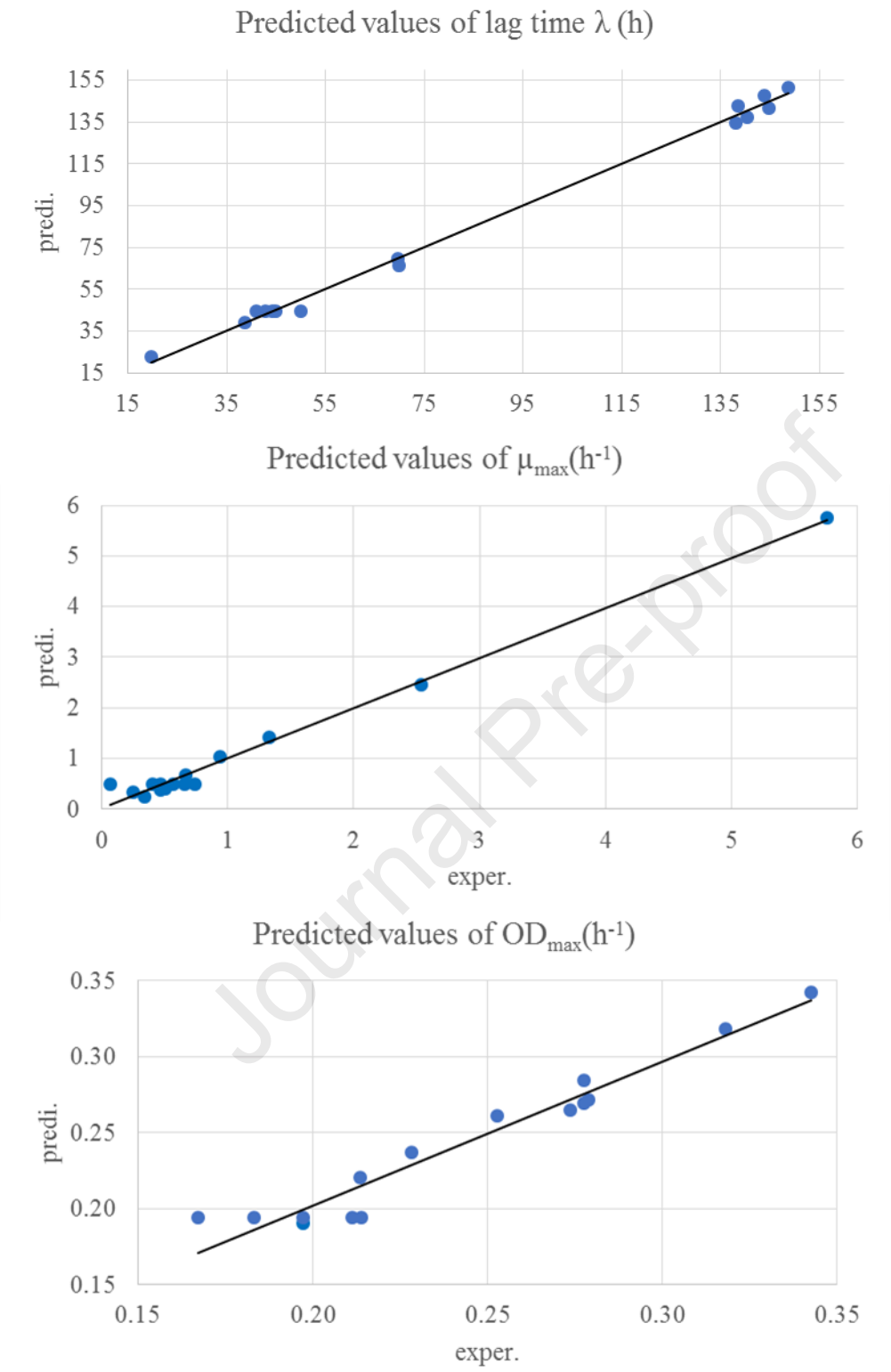

562

563 **Figure 3:** Predicted values of responses using the Baranyi and Roberts model for latency
564 period, λ, the maximum specific growth rate of *E. coli*, μ_{max}, and the maximum optical
565 density, OD_{max}.

566

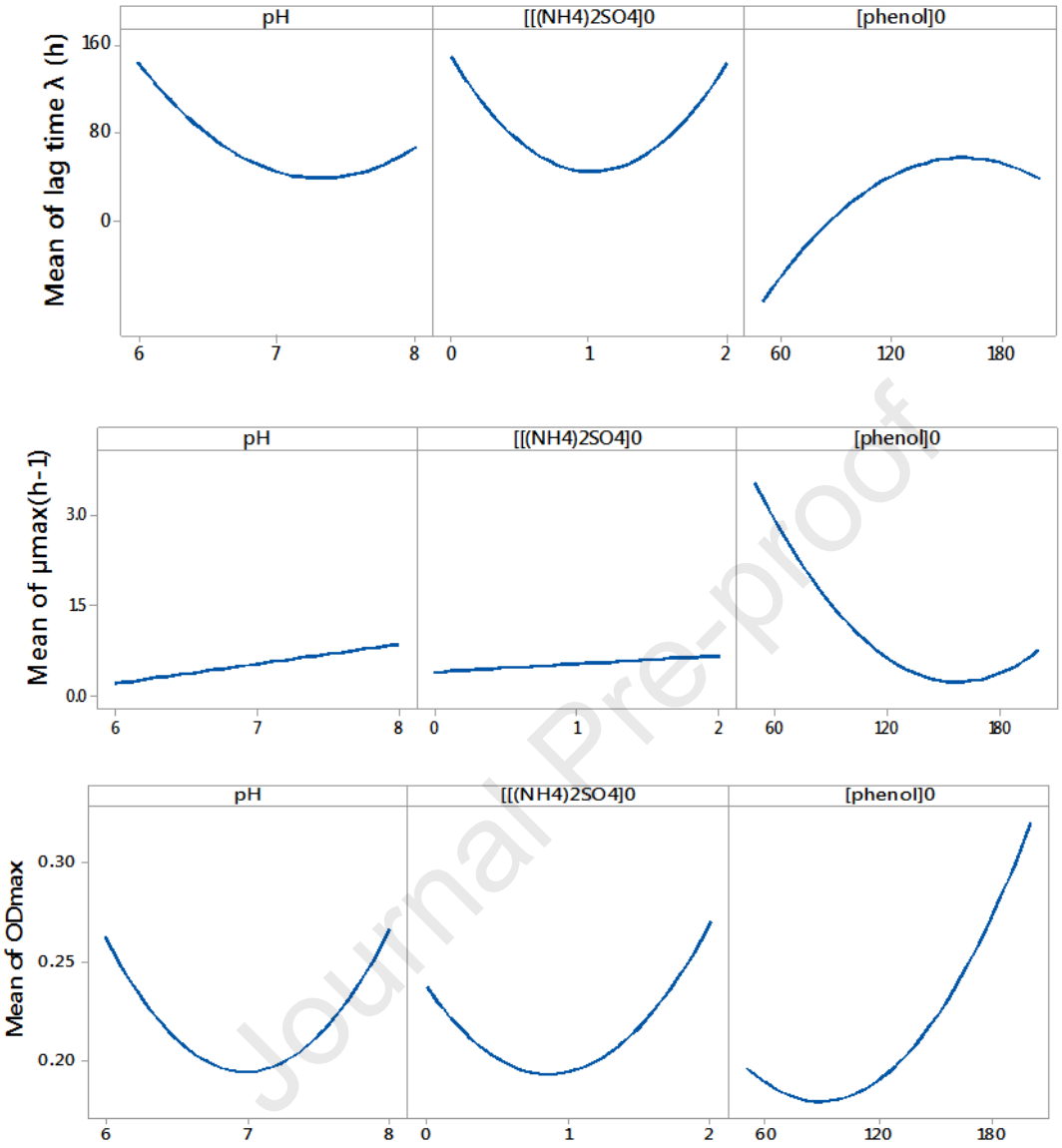

567

568 **Figure 4:** Main effects plot of mean latency time, λ, maximum specific growth rate, μ_{max}, and

569 maximum optical density, OD_{max}.

570

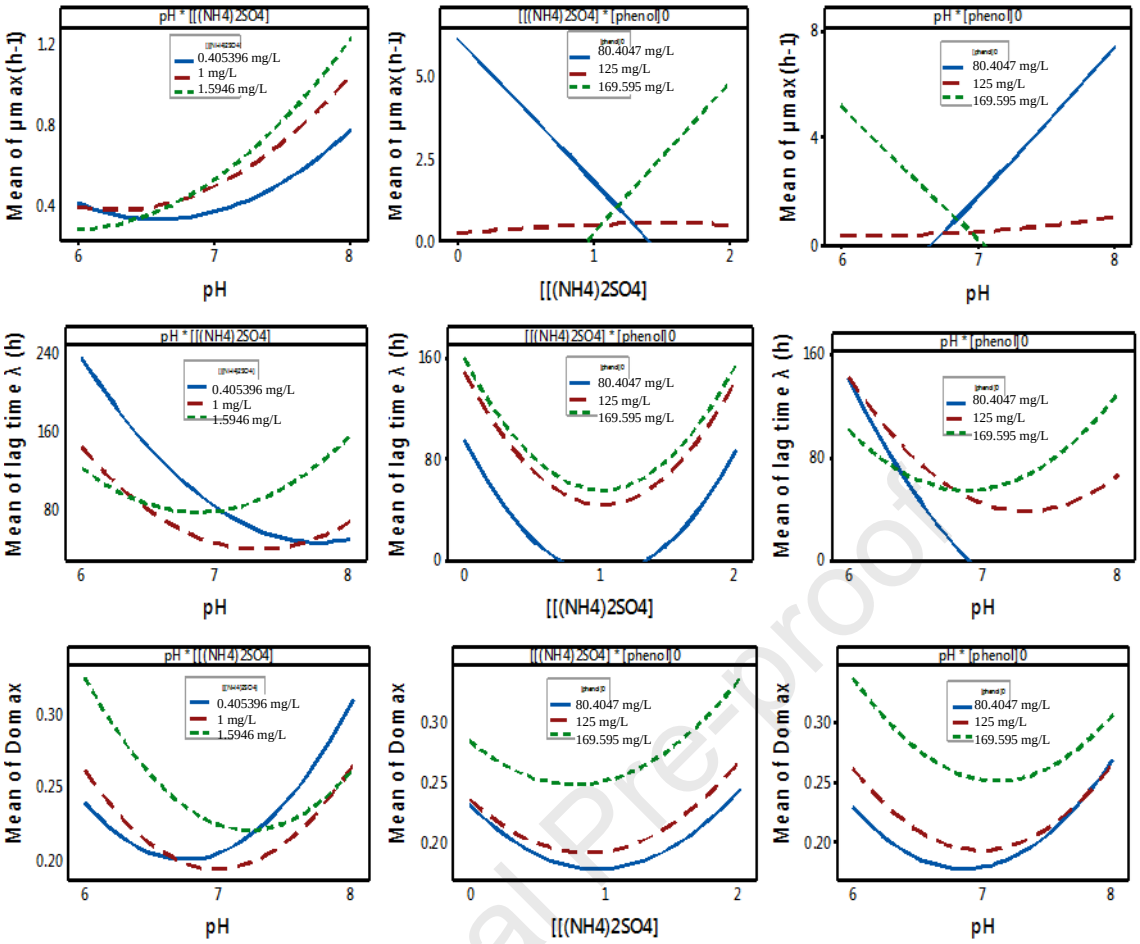

571
572

573 **Figure 5:** Plots of interaction effects for latency time, λ, maximum specific growth rate, μ_{max},

574 and maximum optical density, OD_{max}.

575

576

577

578

579

580

581

582

583

584

585

586

587

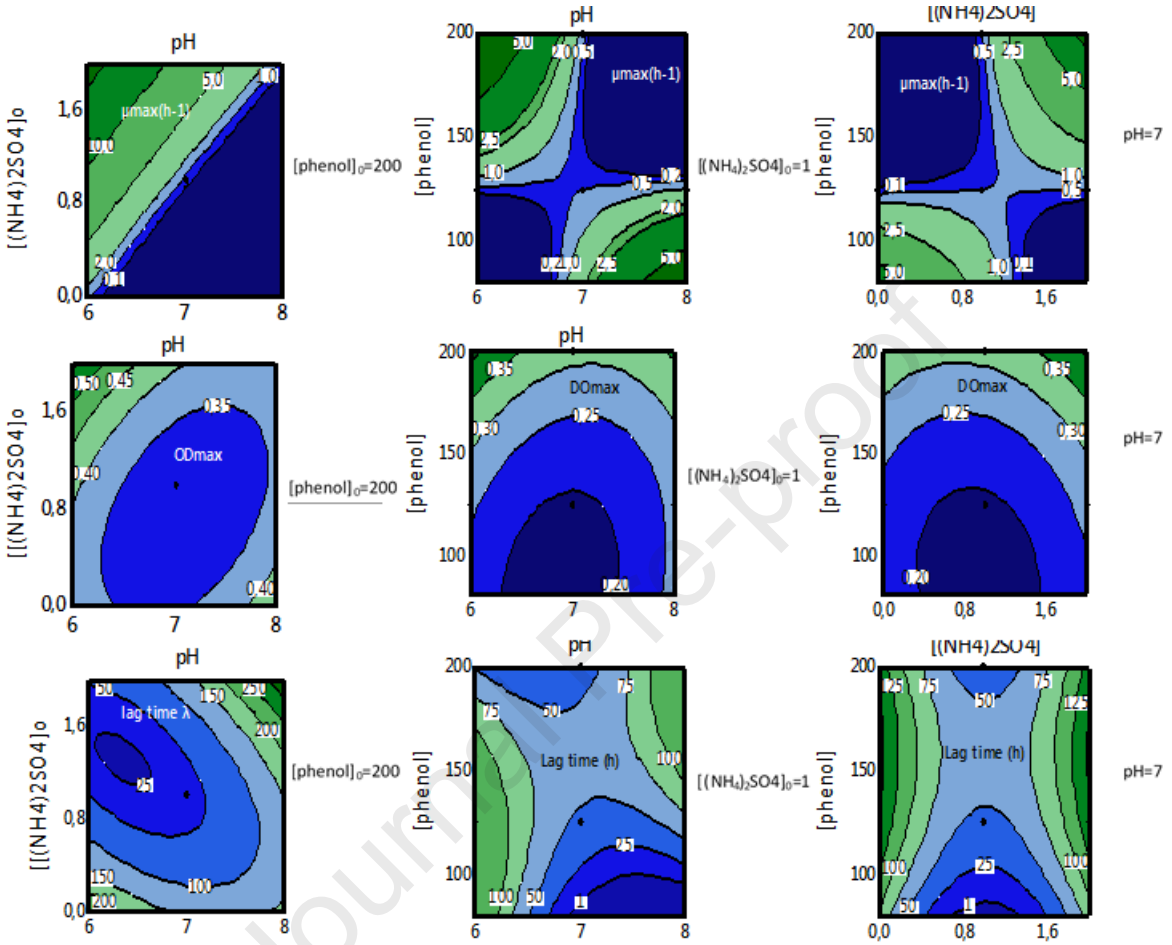

588

589 **Figure 6:** Contour plots for the three responses showing latency time, λ, maximum specific

590 growth rate, μ_{max}, and maximum optical density, OD_{max}.

591

592

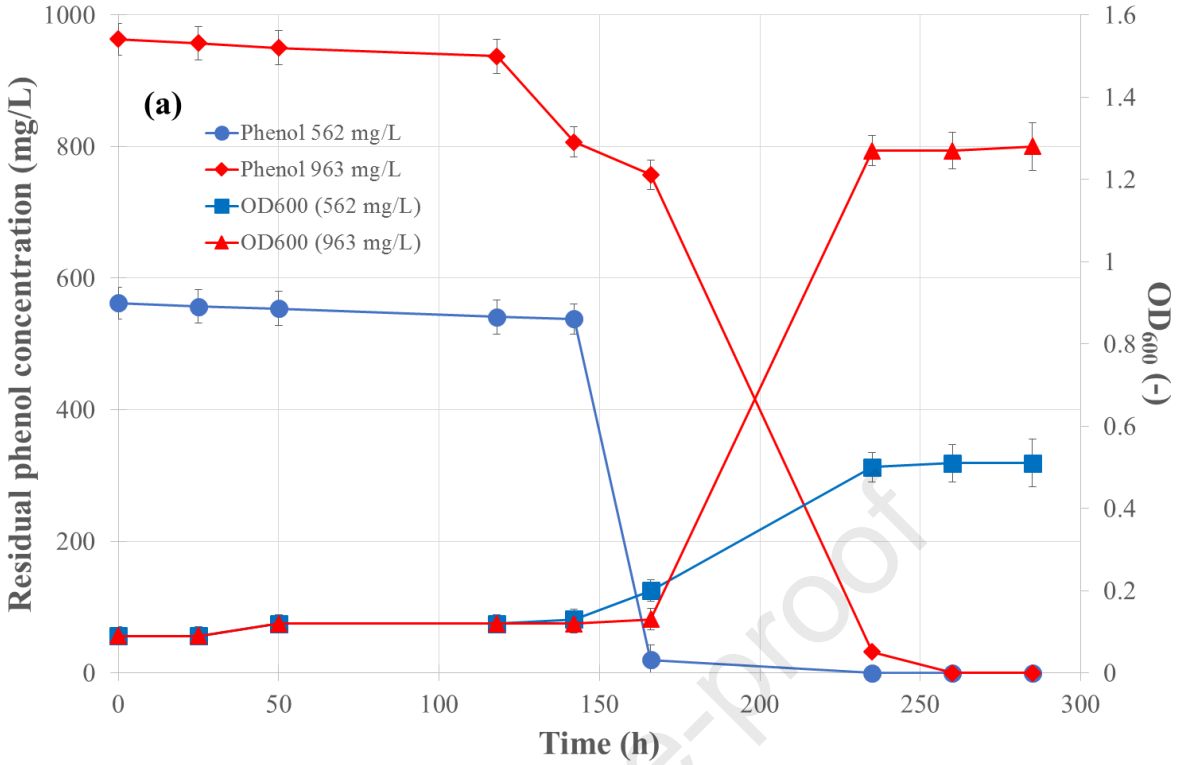

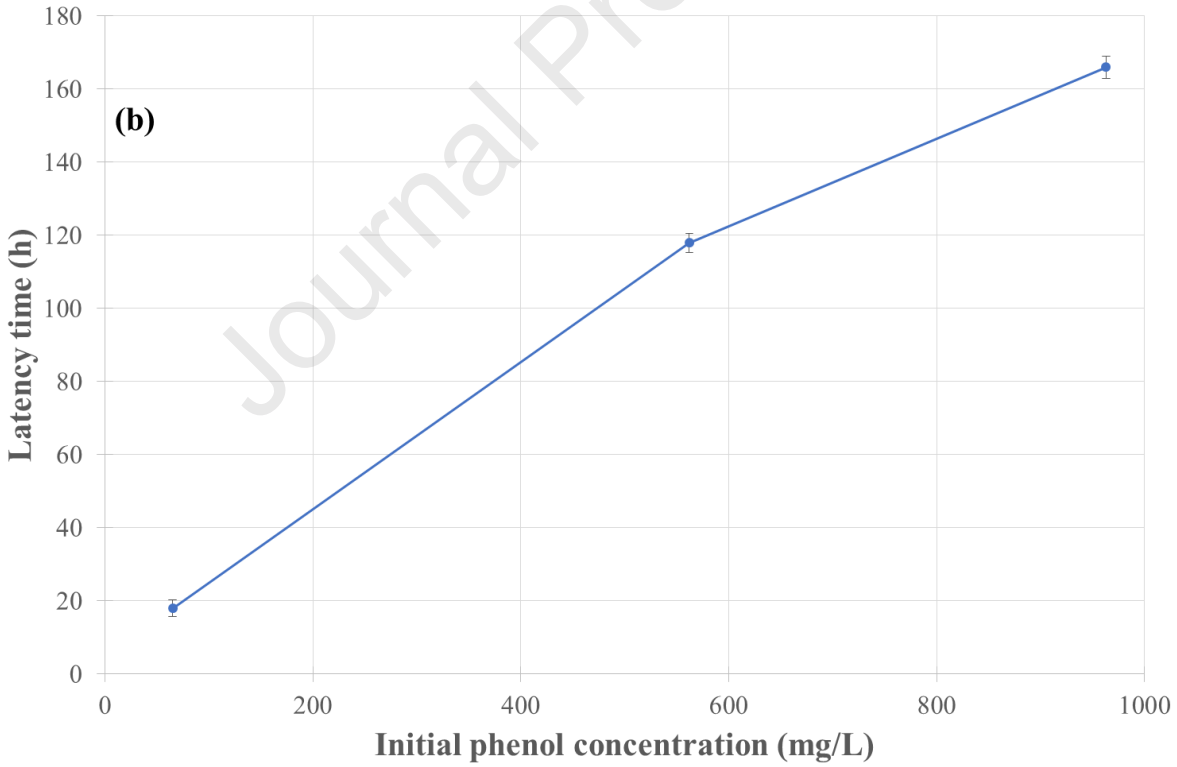

Figure 7: (a) Residual concentration of phenol and optical density as a measurement of bacterial growth as a function of time. (b) Effect of the initial phenol concentration on the latency time.

598

599 **Table 1:** Analysis of variances for the Gompertz and Baranyi and Roberts primary models.

Model		Gompertz	Baranyi and Roberts
Run 1: pH = 6.4, $[(NH_4)_2SO_4]_0$ = 0.405, $[phenol]_0$ = 80.4	RMSE	0.0799	0.0526
	R^2adj	0.9257	0.9678
Run 4: pH = 7.6, $[(NH_4)_2SO_4]_0$ = 1.59, $[phenol]_0$ = 80.4	RMSE	0.0527	0.0526
	R^2adj	0.9747	0.9748
Run 5: pH = 6.4, $[(NH_4)_2SO_4]_0$ = 0.405, $[phenol]_0$ = 170	RMSE	0.0671	0.0681
	R^2adj	0.9454	0.9438
Run 7: pH = 6.4, $[(NH_4)_2SO_4]_0$ = 1.59, $[phenol]_0$ = 170	RMSE	0.1524	0.1524
	R^2adj	0.9562	0.9562
Run 8: pH = 7.6, $[(NH_4)_2SO_4]_0$ = 1.59, $[phenol]_0$ = 170	RMSE	0.0667	0.0672
	R^2adj	0.9528	0.9520
Run 9: pH =6.0, $[(NH_4)_2SO_4]_0$ = 1.00, $[phenol]_0$ = 125	RMSE	0.0945	0.0924
	R^2adj	0.9329	0.9359
Run10: pH = 8.0, $[(NH_4)_2SO_4]_0$ = 1.00, $[phenol]_0$ = 125	RMSE	0.1021	0.1036
	R^2adj	0.9556	0.9544
Run11: pH = 7.0, $[(NH_4)_2SO_4]_0$ = 0, $[phenol]_0$ = 125	RMSE	0.0747	0.0742
	R^2adj	0.9320	0.9328
Run12: pH = 7.0, $[(NH_4)_2SO_4]_0$ = 2.00, $[phenol]_0$ = 125	RMSE	0.0734	0.0780
	R^2adj	0.9284	0.9193
Run 14: pH = 7.0, $[(NH_4)_2SO_4]_0$ = 1, $[phenol]_0$ = 200	RMSE	0.0785	0.0786
	R^2adj	0.9857	0.9856
Run 0: pH = 8, $[(NH_4)_2SO_4]_0$ = 1, $[phenol]_0$ = 125	RMSE	0.2222	0.2218
	R^2adj	0.6616	0.6629
	Lack of fit (*P*-value)	0.6360	0.6570

600
601
602

603 **Table 2:** Experimental range for a central composite rotatable design

Parameters		Coded values				
		–1.68	–1	0	1	1.68
X1	pH	6.0	6.4	7.0	7.6	8.0
X2	$[(NH_4)_2SO_4]_0$, g/L	0	0.4	1.0	1.6	2.0
X3	$[phenol]_0$, mg/L	50.0	80.4	125	170	200

604

605 **Table 3:** Matrix of experiments with coded and non-coded factors

	Coded parameters			Non coded parameters		
Run	X1	X2	X3	pH	$[(NH_4)_2SO_4]_0$	$[phenol]_0$
1	–1	–1	–1	6.4	0.4	80.4
2	1	–1	–1	7.6	0.4	80.4
3	–1	1	–1	6.4	1.6	80.4
4	1	1	–1	7.6	1.6	80.4
5	–1	–1	1	6.4	0.4	170.0
6	1	–1	1	7.6	0.4	170.0
7	–1	1	1	6.4	1.6	170.0
8	1	1	1	7.6	1.6	170.0
9	–1.68	0	0	6.0	1.0	125.0
10	1.68	0	0	8.0	1.0	125.0
11	0	–1.68	0	7.0	0.0	125.0
12	0	1.68	0	7.0	2.0	125.0
13	0	0	–1.68	7.0	1.0	50.0
14	0	0	1.68	7.0	1.0	200.0
15	0	0	0	7.0	1.0	125.0
16	0	0	0	7.0	1.0	125.0
17	0	0	0	7.0	1.0	125.0
18	0	0	0	7.0	1.0	125.0
19	0	0	0	7.0	1.0	125.0

606

607

608 **Table 4:** Estimated Coefficients (coded units) and their *P*-values

Parameters	μ_{max} **(h^{-1})**		λ **(h)**		OD_{max}	
Term	Coef	*P*-Value	Coef	*P*-Value	Coef	*P*-Value
Constant	0.501	0.008	44.55	0.000	0.19456	0.000
pH	0.1912	0.094[a]	–22.64	0.000	0.00117	0.876[a]
$[(NH_4)_2SO_4]_0$	0.0793	0.432[a]	–1.82	0.304[a]	0.00961	0.234[a]
$[phenol]_0$	–0.787	0.002	32.88	0.000	0.0364	0.015
$[pH]^2$	0.0775	0.364[a]	21.15	0.000	0.02427	0.01
$[(NH_4)_2SO_4]_0^2$	–0.046	0.58[a]	35.31	0.000	0.02063	0.018
$[phenol]_0^2$	0.528	0.009	–21.57	0.000	0.02206	0.075[a]
$pH*[(NH_4)_2SO_4]_0$	0.086	0.688[a]	32.16	0.000	–0.0197	0.257[a]
$pH*[phenol]_0$	–2.967	0.000	31.6	0.000	–0.0104	0.568[a]
$[(NH_4)_2SO_4]_0*[phenol]_0$	2.718	0.000	0.44	0.924[a]	0.006	0.74[a]

609 [a] *P*-values (underlined) indicate that the corresponding coefficient is not significant.

610

611 **Table 5:** Analysis of variance for the secondary models (the first three responses are based on
612 the Baranyi and Roberts primary model)

Parameters →	μ_{max} (h^{-1})	λ (h)	OD_{max} (-)
Source of variation		*P*-Value	
Model	0.000	0.000	0.012
Linear	0.007	0.000	0.054[a]
Square	0.037	0.000	0.024
2-Way Interaction	0.000	0.000	0.312[a]
Lack-of-Fit	0.375[a]	0.113[a]	0.325[a]
R^2 (%)	98.8	99.6	94.5

613 [a] *P*-values (underlined) indicate that the corresponding coefficient is not significant.

614

615

- Biodegradation process of phenol in a batch reactor using *Escherichia coli*.
- Optimization of the growth parameters thanks to Baranyi and Roberts'equations
- Optimization of experimental conditions using secondary models based on a central composite rotatable design
- Degradation up to 963 mg/L of phenol in 250 h without acclimatization of *Escherichia Coli*.

Conflict of interest: The authors declare that they have no conflicts of interest.